

# Inorganic polyphosphate is a potent activator of the mitochondrial permeability transition pore in cardiac myocytes

Lea K. Seidlmayer,<sup>1</sup> Maria R. Gomez-Garcia,<sup>2</sup> Lothar A. Blatter,<sup>1</sup> Evgeny Pavlov,<sup>3</sup> and Elena N. Dedkova<sup>1</sup>

<sup>1</sup>Department of Molecular Physiology and Biophysics, Rush University Medical Center, Chicago, IL 60612

<sup>2</sup>Department of Plant Biology, Carnegie Institution for Science, Stanford, CA 94305

<sup>3</sup>Department of Physiology and Biophysics, Dalhousie University, Halifax, NS B3H 3J5, Canada

Mitochondrial dysfunction caused by excessive  $\text{Ca}^{2+}$  accumulation is a major contributor to cardiac cell and tissue damage during myocardial infarction and ischemia–reperfusion injury (IRI). At the molecular level, mitochondrial dysfunction is induced by  $\text{Ca}^{2+}$ -dependent opening of the mitochondrial permeability transition pore (mPTP) in the inner mitochondrial membrane, which leads to the dissipation of mitochondrial membrane potential ( $\Delta\Psi_m$ ), disruption of adenosine triphosphate production, and ultimately cell death. Although the role of  $\text{Ca}^{2+}$  for induction of mPTP opening is established, the exact molecular mechanism of this process is not understood. The aim of the present study was to test the hypothesis that the adverse effect of mitochondrial  $\text{Ca}^{2+}$  accumulation is mediated by its interaction with inorganic polyphosphate (polyP), a polymer of orthophosphates linked by phosphoanhydride bonds. We found that cardiac mitochondria contained significant amounts ( $280 \pm 60 \text{ pmol/mg}$  of protein) of short-chain polyP with an average length of 25 orthophosphates. To test the role of polyP for mPTP activity, we investigated kinetics of  $\text{Ca}^{2+}$  uptake and release,  $\Delta\Psi_m$  and  $\text{Ca}^{2+}$ -induced mPTP opening in polyP-depleted mitochondria. polyP depletion was achieved by mitochondria-targeted expression of a polyP-hydrolyzing enzyme. Depletion of polyP in mitochondria of rabbit ventricular myocytes led to significant inhibition of mPTP opening without affecting mitochondrial  $\text{Ca}^{2+}$  concentration by itself. This effect was observed when mitochondrial  $\text{Ca}^{2+}$  uptake was stimulated by increasing cytosolic  $[\text{Ca}^{2+}]$  in permeabilized myocytes mimicking mitochondrial  $\text{Ca}^{2+}$  overload observed during IRI. Our findings suggest that inorganic polyP is a previously unrecognized major activator of mPTP. We propose that the adverse effect of polyphosphate might be caused by its ability to form stable complexes with  $\text{Ca}^{2+}$  and directly contribute to inner mitochondrial membrane permeabilization.

## INTRODUCTION

Myocardial infarction is caused by sudden loss of blood supply to the heart, leading to ischemic damage of cardiac tissue (Ferreira, 2010a,b). This results in oxygen deprivation (ischemia) causing damage or death of heart muscle tissue. The treatment requires procedures that allow the rapid return of blood flow to the ischemic zone of the myocardium, i.e., reperfusion therapy. Although therapeutically the return of blood supply to the infarcted tissue is of great importance, reperfusion itself is known to cause additional complications, such as diminished cardiac contractile function and arrhythmia,

and to lead to irreversible cell injury, known as ischemia–reperfusion injury (IRI). Thus, minimization of IRI is an important part of clinical strategies to reduce myocardial damage after myocardial infarction.

It is widely recognized that loss of mitochondrial function is a central event leading to tissue damage and cell death in connection with IRI (Halestrap, 2009a; Camara et al., 2011). A large body of experimental data indicates that mitochondrial dysfunction during IRI is caused by a dramatic increase in permeability of the inner mitochondrial membrane caused by the opening of the large nonselective permeability transition pore (mitochondrial permeability transition pore [mPTP]) (Bernardi et al., 2006; Halestrap, 2009a). mPTP opening leads to dissipation of mitochondrial membrane potential ( $\Delta\Psi_m$ ), mitochondrial swelling, and rupture of the outer mitochondrial membrane (Ricchelli et al., 2011). This results in collapse of energy production and release of mitochondrial proapoptotic factors, followed

Correspondence to: Elena N. Dedkova: [Elena\\_Dedkova@rush.edu](mailto:Elena_Dedkova@rush.edu)

Part of this work has been presented in abstract form (Seidlmayer, L., B. Winkfein, L.A. Blatter, E. Pavlov, and E.N. Dedkova. 2010. Biophysical Society 54th Annual Meeting. Abstr. 1957; Seidlmayer, L.K., L.A. Blatter, E. Pavlov, and E.N. Dedkova. 2010. American Heart Association. Abstr. 17373; Seidlmayer, L.K., L.A. Blatter, E. Pavlov, and E.N. Dedkova. 2011. Biophysical Society 55th Annual Meeting. Abstr. 232).

Abbreviations used in this paper: CsA, cyclosporine A; DAPI, 4', 6-diamidino-2-phenylindole, dihydrochloride;  $\Delta\Psi_m$ , mitochondrial membrane potential; ECC, excitation–contraction coupling; IRI, ischemia–reperfusion injury; mPTP, mitochondrial permeability transition pore; PHB, poly- $\beta$ -hydroxybutyrate; P<sub>i</sub>, orthophosphate; polyP, inorganic polyphosphate; PPX, exopolyphosphatase; TMRM, tetramethylrhodamine methyl ester.

© 2012 Seidlmayer et al. This article is distributed under the terms of an Attribution-Noncommercial-Share Alike-No Mirror Sites license for the first six months after the publication date (see <http://www.rupress.org/terms>). After six months it is available under a Creative Commons License (Attribution-Noncommercial-Share Alike 3.0 Unported license, as described at <http://creativecommons.org/licenses/by-nc-sa/3.0/>).

by cell death by either necrotic or apoptotic mechanisms (Rasola and Bernardi, 2011).

It is recognized that excessive  $\text{Ca}^{2+}$  accumulation inside mitochondria is one of the key factors responsible for mPTP opening during IRI (Bernardi et al., 2006; Halestrap, 2009a; Rasola and Bernardi, 2011; Ricchelli et al., 2011). However, details of the molecular nature of mPTP and the mechanisms of induction of pore opening remain poorly understood. Our previous study conducted with stable mammalian cell lines and neuronal cultures identified mitochondrial inorganic polyphosphate (polyP) as a potent mediator of the process of  $\text{Ca}^{2+}$ -induced cell death, suggesting a role in mPTP regulation (Abramov et al., 2007); however, the presence of polyP in cardiomyocytes and its effect on mPTP activity have never been investigated. polyP is an inorganic polymer of multiple orthophosphates linked together by phosphoanhydride bonds (Wood and Clark, 1988; Kornberg et al., 1999; Kulaev et al., 1999). In mammalian organisms, typical lengths of polyP polymers are in the range of 10–100 orthophosphate ( $\text{P}_i$ ) groups. In striking contrast to inorganic phosphate, a known inducer of mPTP (Hunter et al., 1976; Di Lisa and Bernardi, 2009), which is present inside of mitochondria in millimolar concentrations (Werkheiser and Bartley, 1957), polyP is found in mammalian cells only in micromolar concentrations (Kumble and Kornberg, 1995; Kornberg et al., 1999), ruling out its ability to buffer matrix  $\text{Ca}^{2+}$ ,  $\text{Mg}^{2+}$ , or pH significantly and suggesting a direct regulatory role. Indeed, a whole range of critical regulatory roles of polyP in mammalian cells has been recently discovered, including regulation of blood coagulation (Müller et al., 2009), gene expression (Müller et al., 2011), cell differentiation (Kawazoe et al., 2008; Morimoto et al., 2010), bone mineralization (Omelon and Grynpas, 2008; Omelon et al., 2009), and ion channel function (Zakharian et al., 2009). In mammalian mitochondria under normal conditions, polyP was suggested to be involved in regulation of the respiratory chain and ATP production (Pavlov et al., 2010). Importantly, it was also demonstrated that polyP is an integral component of an ion channel extracted from liver mitochondria with properties similar to mPTP (Pavlov et al., 2005b). However, the current understanding of the role of polyP in mammalian mitochondria is limited and has not been studied in cardiac mitochondria. Therefore, the aim of this study was to investigate the relationship between polyP and mPTP opening in cardiac myocytes. We found that: (a) cardiac mitochondria contain significant amounts of polyP; (b) depletion of mitochondrial polyP does not affect cytosolic  $\text{Ca}^{2+}$  cycling, excitation-contraction coupling (ECC), and mitochondrial  $\text{Ca}^{2+}$  transport; however, (c) depletion of polyP inhibits  $\text{Ca}^{2+}$ -induced mPTP opening in cardiomyocytes. These data demonstrate that polyP is a previously unrecognized critical activator of mPTP in cardiac cells and that reduction of polyP can be cardioprotective by preventing mPTP opening.

## MATERIALS AND METHODS

### Cell isolation and culture

Left ventricular myocytes were isolated from adult New Zealand white rabbits (2.5 kg; 3–4 mo old; Myrtle's Rabbitry). Rabbits were anaesthetized with 50 mg  $\text{kg}^{-1}$  sodium pentobarbital, and hearts were excised and mounted on a Langendorff apparatus. Hearts were retrogradely perfused with nominally  $\text{Ca}^{2+}$ -free Tyrode solution for 5 min, followed by Eagle's minimum essential medium (MEM) solution containing 20  $\mu\text{M}$   $\text{Ca}^{2+}$  and 45  $\mu\text{g ml}^{-1}$  Liberase Blendzyme TH (Roche) for 20 min at 37°C. The left ventricular free wall was removed from the heart and digested for an additional 5 min in the enzyme solution at 37°C. Digested tissue was then minced, filtered, and washed in an MEM solution containing 50  $\mu\text{M}$   $\text{Ca}^{2+}$  and 10  $\text{mg ml}^{-1}$  bovine serum albumin. Isolated cells were kept in MEM solution with 50  $\mu\text{M}$   $\text{Ca}^{2+}$  at room temperature (22–24°C) until they were used for culturing. Myocytes were cultured on laminin-covered glass coverslips in PC-1 medium. Experiments were performed 24 h after infection with GFP- or exopolyphosphatase (PPX)-expressing adenoviruses. All protocols were in accordance with the Guide for the Care and Use of Laboratory Animals published by the National Institutes of Health and approved by the institutional Animal Care and Use Committee.

### Mitochondria isolation from rabbit hearts

The mitochondria isolation protocol was based on several previously published methods with slight modifications (Meta and Seitz, 1979; Aon et al., 2010). In brief, a 2.5-kg-weight rabbit was anaesthetized with 50 mg  $\text{kg}^{-1}$  sodium pentobarbital, and the heart was quickly excised. The following procedures were performed on ice. The heart was immediately immersed into ~20 ml of isolation solution (IS) containing 75 mM sucrose, 225 mM mannitol, and 0.01 mM EGTA, pH 7.4 (buffered with Trizma; Sigma-Aldrich). After washing, the portion of the heart with the aorta, the pulmonary arteries, and the atria was discarded. The remaining tissue was immersed into 40 ml of fresh IS and minced. After the tissue pieces settled, the supernatant was discarded, fresh IS (20 ml) was added, and the mixture was transferred to a 50-ml-capacity homogenization vessel. 3.2 mg proteinase (bacterial; type XXIV, formerly called Nagarse; Sigma-Aldrich) was added immediately before starting the homogenization procedure. The heart tissue was homogenized in IS buffer with a Polytron-type tissue grinder at 11,000 rpm for 2.5 s, followed by five to six quick strokes at 500 rpm with a loose-fit tissue grinder (Potter-Elvehjem; LabGlass). To remove red blood cells, unbroken cells, cell membranes, nuclei, and other debris, the homogenate was transferred into two 50-ml centrifuge tubes and centrifuged at 480  $\text{g}$  (2,000 rpm) for 5 min. The supernatant was centrifuged immediately at 7,700  $\text{g}$  (8,000 rpm) for 10 min. The supernatant was discarded, and the pellets were rinsed with cold IS. With a small amount of medium (2–3 ml) in the tube, the fluffy layer on top of the pellets was shaken loose and discarded. Then, the mitochondrial pellets were resuspended with 15 ml of cold IS and centrifuged at 7,700  $\text{g}$  (8,000 rpm) for 5 min. The washing procedure, including rinsing the surface of the pellet, resuspending the mitochondria, and centrifugation, was repeated twice using suspension solution (IS without EGTA). When the final mitochondrial pellet was obtained, the supernatant was discarded, the pellet surface was rinsed once more, and the mitochondria were resuspended in 1 ml of suspension solution. Mitochondrial protein concentration was determined by protein assay (Bradford, 1976) (Pierce BCA; Thermo Fisher Scientific), yielding on average 5 mg of mitochondrial protein/ml (5 mg of total protein) from one rabbit heart. Respiratory control ratios (ratio of state 3 over state 4 respiration with glutamate plus malate) of 6–8 were obtained using this method. All isolation procedures were performed on wet ice.

### polyP extraction, quantification, and size determination

polyP was extracted using a modified phenol/chloroform extraction protocol (Kumble and Kornberg, 1995). The mitochondrial pellet (see above) was resuspended in 250  $\mu$ l TELS buffer (100 mM LiCl, 10 mM EDTA, and 10 mM Tris, pH 8.0, 0.5% SDS) and mixed with 250  $\mu$ l of acid phenol/chloroform, pH 4.5 (with isooamyl alcohol [IAA]; acid phenol/chloroform/IAA [125:24:1]; Invitrogen). 425–600- $\mu$ m glass beads (Sigma-Aldrich) were added to the level right below the phenol fraction for extraction of polyP associated with the membrane fraction. Samples were vortexed for 5 min at 4°C, followed by centrifugation at 1,500 g for 5 min at 4°C. The water phase was transferred to a new tube and subjected to chloroform extraction with the equal volume of chloroform to remove traces of organic solvents from the water phase. polyP was precipitated from the water phase by adding 2.5 volumes of ethanol, followed by overnight incubation at –20°C. The water–ethanol mixture was centrifuged for 10 min at 10,000 g. The resulting pellet containing polyP was resuspended in 50  $\mu$ l of a buffer (0.1% SDS, 1 mM EDTA, and 10 mM Tris-HCl, pH 7.4) treated with RNase and DNase to remove nucleic acid contamination and loaded on a 30% polyacrylamide gel prepared in the following solution (in mM): 90 Tris-KOH, pH 8.3, 90 boric acid, and 2.7 EDTA in the presence of 7 M urea. A gel size of 70 cm was run for 30 min at 80 V, followed by 6 h at 40 V. polyP was visualized by DAPI staining (Smith and Morrissey, 2007). polyP with an average size of 25 orthophosphates (polyP 25; Sigma-Aldrich) was used as standard. The amount of polyP extracted from mitochondrial samples was estimated from the amount of  $P_i$  released upon treatment with recombinant PPX from yeast (*Saccharomyces cerevisiae* PPX) in the reaction mixture containing (in mM): 100 Tris-HCl, pH 7.5, 50 ammonium acetate, 5 magnesium acetate, and PPX in excess to ensure complete polyP hydrolysis.  $P_i$  released after PPX treatment was quantified colorimetrically using the Fiske-Subbarow method (Fiske and Subbarow, 1925). In brief, 50  $\mu$ l of the samples was mixed with 500  $\mu$ l of 2.5% solution of ammonium molybdate prepared in 5 N sulfuric acid and 50  $\mu$ l Fiske-Subbarow reagent (Sigma-Aldrich), with the total volume adjusted to 1 ml with water. The amount of  $P_i$  was estimated by the optical density of the solution at 650 nm and compared with the standard  $P_i$  solution (Sigma-Aldrich).

### polyP depletion in mitochondria

To decrease the amount of polyP in mitochondria, mitochondrial-targeted GFP-tagged PPX (Abramov et al., 2007) that specifically hydrolyzes polyP into inorganic phosphate was adenovirally expressed in cardiac myocytes. The adenoviral construct (MTS-GFP) expressed GFP together with a mitochondrial targeting sequence derived from the precursor of subunit VIII of human cytochrome c oxidase. Control cells were infected with an adenoviral vector that contained only the DNA for GFP without PPX. polyP levels were estimated in myocytes infected with PPX or GFP adenoviruses after 24 h in culture.

### Permeabilized ventricular myocytes

The sarcolemma was permeabilized with digitonin (10  $\mu$ M for 60 s) as described previously (Sedova et al., 2006; Dedkova and Blatter, 2009). Digitonin was added to the intracellular solution containing (in mM): 135 KCl, 10 NaCl, 20 HEPES, 5 pyruvate, 2 glutamate, 2 malate, 0.5  $KH_2PO_4$ , 0.5  $MgCl_2$ , 15 2,3-butanedione monoxime, 5 EGTA, and 1.86  $CaCl_2$  to yield a free  $[Ca^{2+}]_i$  of 100 nM with pH 7.2. After permeabilization, the bath solution was changed to the same intracellular solution but without digitonin.

### Fluorescence measurements

Laser scanning confocal microscopy (A1R; Nikon) was used to follow the changes in polyP concentration, cytosolic  $[Ca^{2+}]_i$ , mitochondrial  $Ca^{2+}$  uptake,  $\Delta\Psi_m$ , and mPTP activity. All fluorescence

signals were background corrected and recorded from individual cells. All fluorescent indicators were obtained from Invitrogen.

### Cytosolic $[Ca^{2+}]$ ( $[Ca^{2+}]_i$ ) measurements

These were performed in intact cells with Indo-1 using an epifluorescence microscopy setup (Ionoptix). Action potentials were triggered at 1 Hz by electrical field stimulation with a pair of platinum electrodes. The electrical stimulus was set at a voltage ~50% greater than the threshold to induce myocyte contraction. Left ventricular myocytes attached to laminin-coated (20  $\mu$ g/ml) coverslips were loaded with 5  $\mu$ M Indo-1/AM in the presence of 0.05% Pluronic F-127 (Invitrogen) for 15 min, washed for 10 min in Tyrode solution to allow for de-esterification of the dye, and then superfused continuously (1 ml/min) with Tyrode solution. Indo-1 was excited at 340 nm, with emission signals simultaneously recorded at 405 nm ( $F_{405}$ ) and 485 nm ( $F_{485}$ ). Changes in  $[Ca^{2+}]_i$  are expressed as changes of the ratio  $R = F_{405}/F_{485}$ .  $Ca^{2+}$  transient amplitudes are presented as  $\Delta R = R_{peak} - R_{diast}$  ( $R_{diast}$ , diastolic  $[Ca^{2+}]$ ).

### polyP levels

These were estimated in intact cells loaded with 5  $\mu$ g/ml 4', 6-diamidino-2-phenylindole, dihydrochloride (DAPI) for 30 min at 37°C (Aschar-Sobbi et al., 2008). DAPI was excited with 408-nm laser light, and emitted fluorescence was measured at 552–617 nm. For DAPI emission spectrum recording, cells were excited at 408 nm, and the emission spectrum was collected between 500 and 675 nm. Data are presented as background subtracted fluorescence in arbitrary fluorescence units collected from the whole cell.

### Mitochondrial matrix $[Ca^{2+}]$ ( $[Ca^{2+}]_m$ ) measurements

These were performed in permeabilized cells loaded with either 5  $\mu$ M of X-Rhod-1/AM or Rhod-2/AM for 30 min at 37°C as described previously (Sedova et al., 2006; Dedkova and Blatter, 2012). In brief, X-Rhod-1 or Rhod-2 was excited with the 543-nm line of a green HeNe laser, and emitted fluorescence was measured at 552–617 nm. Mitochondrial X-Rhod-1 or Rhod-2 fluorescence intensity (F) in each experiment was normalized to the level of fluorescence recorded before stimulation ( $F_0$ ) but after cell permeabilization. Changes in  $[Ca^{2+}]_m$  are expressed as  $\Delta F/F_0$ , where  $\Delta F = F - F_0$ .

### Measurement of $\Delta\Psi_m$

Changes in  $\Delta\Psi_m$  were followed using the potential-sensitive dye tetramethylrhodamine methyl ester (TMRM;  $\lambda_{ex} = 543$  nm and  $\lambda_{em} = 552$ –617 nm) (Dedkova and Blatter, 2005, 2012). Cells were exposed to 5 nM TMRM for 30 min at 37°C before experiments, and then permeabilized with digitonin as described above (Dedkova and Blatter, 2009). All solutions contained 5 nM TMRM during recordings. The decrease in TMRM fluorescence reflects depolarization of the mitochondrial membrane. At the end of each experiment, 1  $\mu$ M FCCP was applied to obtain the minimal signal (maximal depolarization) required for fluorescence normalization.

### Activity of mPTP

This was monitored in permeabilized cells loaded with 5  $\mu$ M calcein red (Invitrogen)/AM ( $\lambda_{ex} = 543$  nm and  $\lambda_{em} = 552$ –617 nm) for 30 min at 37°C. Opening of the mPTP resulted in a decrease of calcein red fluorescence caused by a loss of mitochondria-entrapped calcein red (790 D) (Petronilli et al., 1999; Dedkova and Blatter, 2009, 2012). At the end of each recording, 10  $\mu$ M of the pore-forming antibiotic alamethicin (Marsh, 1996) or alamethicin in combination with digitonin (10  $\mu$ M each) was applied to provide a control measure for maximum calcein red release from mitochondria and to obtain a minimum intracellular calcein red fluorescence level required for signal normalization. Loss of mitochondrial calcein red induced by elevating  $[Ca^{2+}]_{em}$  (2  $\mu$ M)

was quantified as percent decrease of the normalized calcine red fluorescence decrease.

#### Statistical analysis

Statistical differences of the data were determined with the Student's *t* test for unpaired data and considered significant at  $P < 0.05$ . Results are reported as means  $\pm$  SEM for the indicated number (*n*) of cells unless stated otherwise.

## RESULTS

**Detection and enzymatic depletion of mitochondrial polyP**  
 Although the presence of polyP is documented for numerous mammalian cell types and species (Kumble and Kornberg, 1995; Kornberg et al., 1999), it has never been measured in cardiac mitochondria. Here, we demonstrate the presence and quantified the amounts of polyP in mitochondria of cardiac cells (rabbit ventricular myocytes). polyP was extracted and purified from isolated cardiac mitochondria (Kumble and Kornberg, 1995). The amount of polyP was quantified using a highly specific enzymatic assay that relies on measurements of  $P_i$  released from the sample upon treatment with recombinant PPX. We estimated that mitochondria contain  $280 \pm 60$  pmol/mg of protein polyP ( $P_i$  units released by PPX treatment) (Fig. 1 A, left). The presence of

polyP was further confirmed by its characteristic distribution on high resolution polyacrylamide gel, where the polyP sample and standard appear as a characteristic "polyphosphate ladder" (Cowling and Birnboim, 1994). The appearance of this ladder is caused by the fact that both polyP standard and polyP sample from mitochondria are in fact composed of a heterogeneous mixture of polymers of various sizes. Each band seen on the gel represents a polyP polymer of a certain size, with every next band representing the polymer that differs by a single  $P_i$  group (Fig. 1 A, right).

The band distribution of the sample was comparable to the band distribution of polyP-25 standard, suggesting that in cardiac mitochondria, the average length of polyP is in the range of 25  $P_i$  residues. Specific depletion of mitochondrial polyP in cardiac cells was achieved by targeted expression of PPX using an adenoviral infection system. Expression of the enzyme was monitored by measuring fluorescence of GFP attached to PPX (Fig. 1 B, top panel). Control cells were infected with a virus carrying DNA encoding for GFP alone. Cells infected with GFP alone demonstrated an evenly distributed fluorescence signal (Fig. 1 B, top left), whereas cells infected with mitochondrially targeted GFP-PPX showed a fluorescence signal localized predominantly to mitochondrial regions (Fig. 1 B, top right). The colocalization of GFP-PPX and TMRM used as a

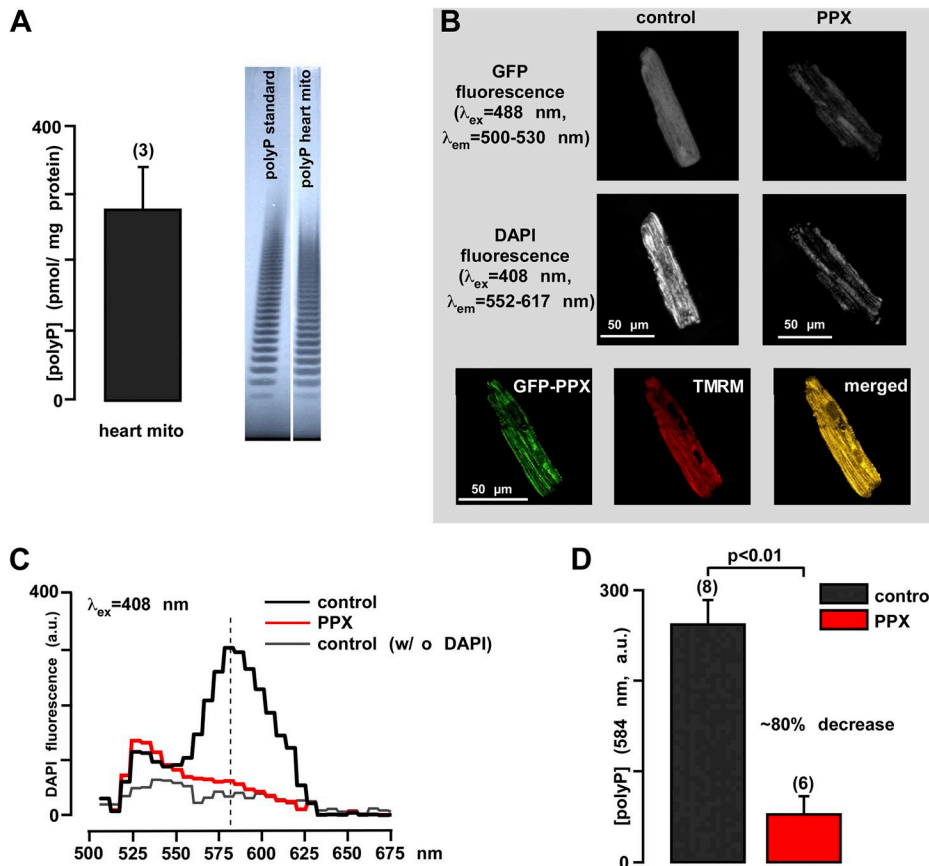


**Figure 1.** polyP detection and manipulation in rabbit heart mitochondria and cardiomyocytes. (A) Average amount of polyP in rabbit heart mitochondria (left) and gel images of polyP standard and polyP sample from isolated rabbit mitochondria (right). (B) Images of control GFP (left) and GFP-PPX-expressing cells (right). The top panel shows global GFP fluorescence at 500–530 nm that reveals the mitochondrial fluorescence pattern in PPX-expressing cells and a homogeneously distributed fluorescence in control cells. The middle panel shows the decrease in DAPI fluorescence in polyP-depleted cells. The bottom panel shows colocalization of GFP-PPX signal with mitochondria. TMRM was used as a mitochondrial signal, and the degree of overlay is presented in shades of yellow in the merged image. (C) Fluorescence spectrum of 5  $\mu$ M of DAPI-loaded myocytes expressing control GFP (black), PPX (red), and control GFP cells not loaded with DAPI (gray). (D) Mean values from the DAPI spectrum obtained in C for GFP (black)- and PPX (red)-expressing myocytes at  $\lambda_{em} = 584$  nm. a.u., arbitrary fluorescence units. The numbers in parenthesis indicate the number of hearts (A) or number of cells (D).

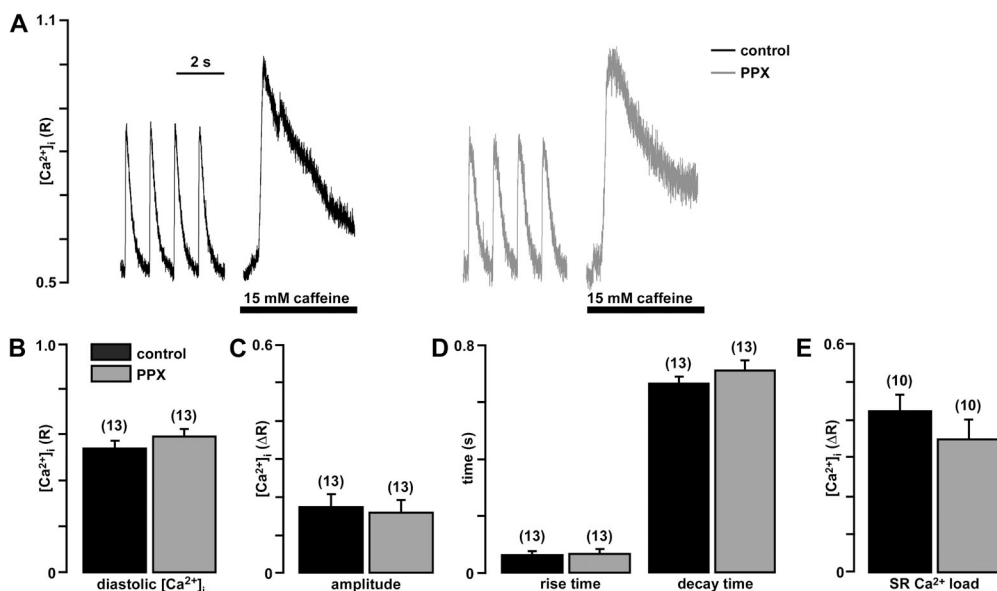


**Figure 2.** Expression of PPX does not alter cardiac ECC. (A) Original recordings of  $[Ca^{2+}]_i$  transients during field stimulation at 1 Hz and caffeine application from cells infected with control GFP virus (black) and PPX virus (gray). (B) Average values of diastolic  $[Ca^{2+}]_i$ . (C) Amplitude of field stimulation-induced  $[Ca^{2+}]_i$  transients. (D) Rise time to 90% peak and decay time to 10% above baseline of electrically stimulated  $[Ca^{2+}]_i$  transients. (E) SR  $Ca^{2+}$  load expressed as average amplitudes of caffeine-induced  $Ca^{2+}$  release. Here and in the subsequent figures, numbers in parenthesis indicate number of cells.

mitochondrial marker is shown in the bottom panel of Fig. 1 B. Relative levels of polyP in control and PPX-expressing cells were estimated by measuring fluorescence intensity of the DAPI–polyP complex (Abramov et al., 2007; Aschar-Sobbi et al., 2008). When excited at 408 nm, control cells showed an emission spectrum with a maximum at 584 nm that is characteristic for the DAPI–polyP complex (Fig. 1 C). Expression of PPX caused a significant ( $\sim 80\%$ ;  $P < 0.01$ ;  $n = 6$ ) decrease in DAPI fluorescence (Fig. 1 B, middle), confirming that mitochondria of these cells underwent a significant depletion of polyP compared with control cells expressing GFP alone (Fig. 1 D). Control cells that were not loaded with DAPI showed no increase in fluorescence (Fig. 1 C). These experiments confirm that PPX can be expressed in cardiac myocytes and that its expression leads to the depletion of mitochondrial  $Ca^{2+}$ .

#### Effect of polyP depletion on cytosolic $Ca^{2+}$ cycling during ECC

In a first set of experiments (Fig. 2), we tested whether mitochondrial polyP depletion altered normal  $Ca^{2+}$  cycling during cardiac ECC. In intact field-stimulated (1 Hz) myocytes, diastolic  $[Ca^{2+}]_i$ , amplitude and kinetics of cytosolic  $[Ca^{2+}]_i$  transients, and  $Ca^{2+}$  content of the SR estimated from the response to the addition of 15 mM caffeine were not affected by depletion of mitochondrial polyP levels, suggesting that the expression of PPX did not have any acute effects on  $Ca^{2+}$  signaling during ECC.

**Effect of polyP depletion on mitochondrial  $Ca^{2+}$  handling**  
We determined whether polyP depletion affected mitochondrial  $Ca^{2+}$  uptake and extrusion. In permeabilized cells,  $Ca^{2+}$  uptake was induced by elevation of the extramitochondrial free  $Ca^{2+}$  concentration ( $[Ca^{2+}]_{em}$ ) from 0.1 to 0.8  $\mu$ M, and  $[Ca^{2+}]_m$  was measured using

the mitochondria  $Ca^{2+}$ -sensitive dye X-rhod-1 (Fig. 3 A). The use of such low  $[Ca^{2+}]_{em}$  was required to prevent the opening of the mPTP caused by excessive intramitochondrial  $Ca^{2+}$  accumulation. Expression of PPX and depletion of mitochondrial polyP did not cause any significant differences in the amount and kinetics of mitochondrial  $Ca^{2+}$  uptake or extrusion (Fig. 3 B).

Next, we studied how polyP depletion affected the susceptibility of mitochondria to  $Ca^{2+}$ -induced mPTP opening. In these experiments, mitochondria of permeabilized

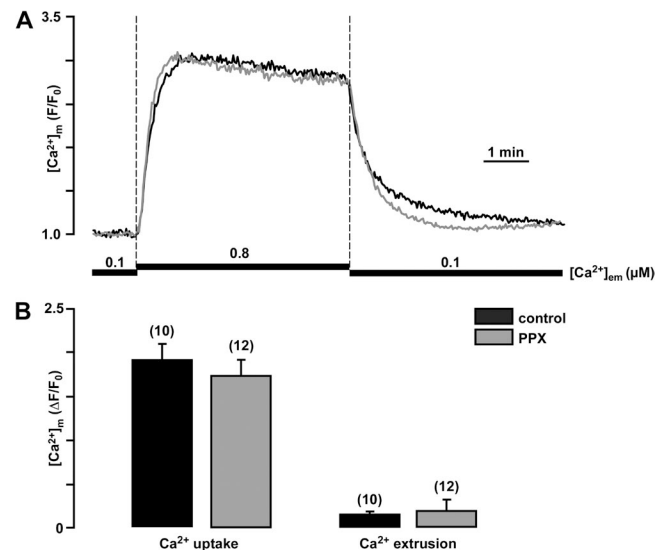


**Figure 3.** Expression of PPX does not alter mitochondrial  $Ca^{2+}$  handling during moderate elevation of  $[Ca^{2+}]_{em}$ . (A) Original recordings of  $[Ca^{2+}]_m$  changes in permeabilized myocytes upon elevation of  $[Ca^{2+}]_{em}$  from 0.1 to 0.8  $\mu$ M, and subsequent return to 0.1  $\mu$ M in control and PPX-infected cells. (B) Average values of mitochondrial  $Ca^{2+}$  uptake (left) and extrusion (right) ( $[Ca^{2+}]_m$  amplitudes measured at 5 min of  $Ca^{2+}$  addition or removal) in control and PPX-expressing cells.

cells were loaded with the  $\text{Ca}^{2+}$  indicator dye X-rhod-1 and exposed to a stepwise increase in  $[\text{Ca}^{2+}]_{\text{em}}$  from 0.1 to 0.8 and to 2  $\mu\text{M}$ . The amplitude of  $[\text{Ca}^{2+}]_{\text{m}}$  was virtually identical in control and PPX-expressing cells when low  $[\text{Ca}^{2+}]_{\text{em}}$  (0.8  $\mu\text{M}$ ) was used to stimulate mitochondrial  $\text{Ca}^{2+}$  uptake (Fig. 4 A). Subsequent exposure to high  $[\text{Ca}^{2+}]_{\text{em}}$  (2  $\mu\text{M}$ ) led to an additional increase in X-Rhod-1 fluorescence in PPX cells (Fig. 4, A and B). However, in control cells, an initial small increase was followed by a significant decline in X-Rhod-1 fluorescence, presumably caused by the release of  $\text{Ca}^{2+}$  and/or X-Rhod-1 dye from mitochondria as a result of mPTP opening (Fig. 4, A and B). Subsequent lowering of  $[\text{Ca}^{2+}]_{\text{em}}$  to 0.1  $\mu\text{M}$  caused a significantly faster decrease in X-Rhod-1 fluorescence in polyP-depleted mitochondria ( $\sim 2.5$  times faster;  $P < 0.05$ ) compared with control mitochondria. This further supports the notion that polyP-depleted but not control mitochondria retained their ability to regulate  $[\text{Ca}^{2+}]_{\text{m}}$ . Similar results were obtained when Rhod-2 was used to measure  $[\text{Ca}^{2+}]_{\text{m}}$  (Fig. 4 C). Elevation of  $[\text{Ca}^{2+}]_{\text{em}}$  in a single step from 0.1 to 2  $\mu\text{M}$  caused a rapid increase of  $[\text{Ca}^{2+}]_{\text{m}}$  that was followed by a steady decline in Rhod-2 fluorescence caused by dye loss via mPTP. The transient increase of the fluorescence signal under control conditions early during exposure to 2  $\mu\text{M}$   $\text{Ca}^{2+}$  likely reflects additional  $\text{Ca}^{2+}$  entry (presumably through the open mPTP) that was followed

by continued loss of indicator dye through the pore, leading to a steady decline of the signal. This transient increase and the decline were significantly attenuated in cyclosporine A (CsA)-treated and/or polyP-depleted cells (Fig. 4 D). The overall kinetics of fluorescence change after polyP depletion were similar to the kinetics of mitochondria treated with the mPTP inhibitor CsA, strongly suggesting the involvement of mPTP (Fig. 4, C and D).

#### polyP depletion prevents $\Delta\Psi_{\text{m}}$ depolarization and opening of mPTP during mitochondrial exposure to high $\text{Ca}^{2+}$

To further confirm that the effects observed with  $\text{Ca}^{2+}$ -sensitive dyes were related to mPTP opening, we measured  $\text{Ca}^{2+}$ -induced changes in  $\Delta\Psi_{\text{m}}$  using the voltage-sensitive dye TMRM in permeabilized myocytes. Monitoring  $\Delta\Psi_{\text{m}}$  with TMRM revealed no differences in basal  $\Delta\Psi_{\text{m}}$  between the two groups; however, an elevation of  $[\text{Ca}^{2+}]_{\text{em}}$  from 0.1 to 2  $\mu\text{M}$   $\text{Ca}^{2+}$  caused a decline of TMRM fluorescence that was significantly more pronounced in control cells compared with polyP-depleted cells (Fig. 5, A and B). Finally, the effect of mPTP inhibition by polyP depletion was confirmed by measurement of mPTP opening using the calcein red assay (Fig. 5, C and D). Mitochondrially entrapped calcein red with a molecular weight of 790 is released from mitochondria only through an open mPTP (maximum

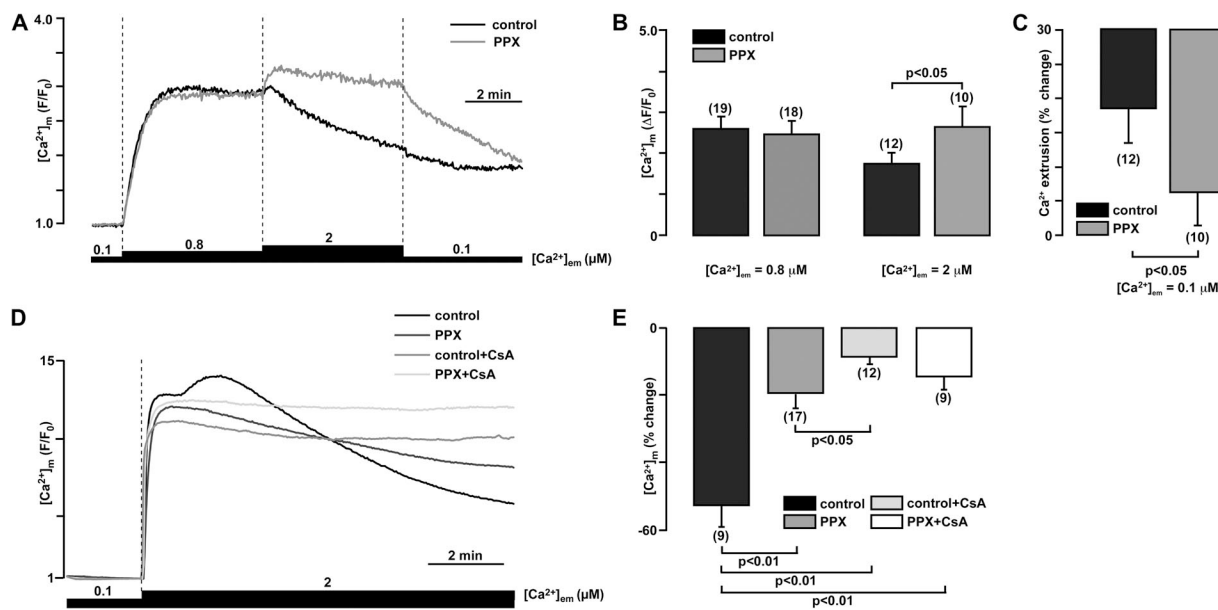


**Figure 4.** Depletion of polyP prevents  $\text{Ca}^{2+}$  release from mitochondria in permeabilized myocytes. (A) Original recordings of  $[\text{Ca}^{2+}]_{\text{m}}$  changes in permeabilized X-Rhod-1-loaded myocytes upon stepwise elevation of  $[\text{Ca}^{2+}]_{\text{em}}$  from 0.1 to 0.8 to 2  $\mu\text{M}$  and subsequent return to 0.1  $\mu\text{M}$  in control (black) and PPX-infected cells (gray). The expression of PPX prevented the release of  $\text{Ca}^{2+}$  from mitochondria during the exposure to 2  $\mu\text{M}$   $\text{Ca}^{2+}$ . (B) Average values for  $[\text{Ca}^{2+}]_{\text{m}}$  amplitude measured at 5 min of 0.8 (left)- and 2- $\mu\text{M}$  (middle)  $\text{Ca}^{2+}$  exposure. (C) Average values for  $\text{Ca}^{2+}$  extrusion upon exposure to 0.1  $\mu\text{M}$   $\text{Ca}^{2+}$  (percent decline normalized to  $[\text{Ca}^{2+}]_{\text{em}}$  levels before exposure to 0.1  $\mu\text{M}$   $\text{Ca}^{2+}$ ; right). (D) Original recordings of  $[\text{Ca}^{2+}]_{\text{m}}$  changes in permeabilized Rhod-2-loaded myocytes upon elevation of  $[\text{Ca}^{2+}]_{\text{em}}$  from 0.1 to 2  $\mu\text{M}$  in control (black), PPX-infected cells (dark gray), CsA-treated control cells (medium gray), and CsA-treated, PPX-infected cells (light gray). (E) Average values of Rhod-2 fluorescence decrease at 10 min after exposure to 2  $\mu\text{M}$   $\text{Ca}^{2+}$ , calculated as a percentage of the initial maximal increase in control, PPX-infected cells, CsA-treated control, and CsA-treated, PPX-infected cells.

size of mPTP permeable compounds is  $\sim$ 1,500 D (Bernardi et al., 2006). As shown in Fig. 5 (C and D), an increase of  $[\text{Ca}^{2+}]_{\text{em}}$  from 0.1 to 2  $\mu\text{M}$  caused calcein red release from mitochondria that was significantly inhibited in both polyP-depleted and CsA-treated mitochondria. The combination of polyP depletion and CsA treatment did not further prevent PTP opening, suggesting that the effect of polyP depletion alone was already maximal. Collectively, these data support the hypothesis that decreased levels of mitochondrial polyP caused a significant inhibition of  $\text{Ca}^{2+}$ -induced mPTP opening.

## DISCUSSION

Opening of the mPTP is the central event in many types of cell and tissue injuries, including cardiac IRI, leading to necrotic and apoptotic cell death (Camara et al., 2011; Rasola and Bernardi, 2011). The mPTP is a highly dynamic, nonselective pore in the inner mitochondrial membrane providing a permeation pathway to ions, solutes, and small proteins (Ricchelli et al., 2011). It is generally accepted that mPTP is a macromolecular complex

that contains several proteins with established regulatory roles for the adenine nucleotide translocase and cyclophilin D (Bernardi et al., 2006; Halestrap, 2009a; Ricchelli et al., 2011). In cardiac myocytes, inhibition of mPTP opening prevents cell death under hypoxic conditions (Halestrap, 2009a; Camara et al., 2011). Several recent clinical trials identified mPTP as a very promising target for protection against or treatment of IRI (Piot et al., 2008; Gomez et al., 2009). Thus, understanding the details of structural organization and regulation of mPTP in cardiac myocytes is critically important for the development of strategies of protection against cardiac tissue damage. However, the molecular mechanism of mPTP activation by  $\text{Ca}^{2+}$  as well as the molecular identity of the channel portion of the mPTP complex has remained elusive. It is known that the sensitivity to matrix  $\text{Ca}^{2+}$  is enhanced by several factors such as oxidative stress, increased levels of inorganic phosphate, and membrane depolarization (Halestrap, 2009a). Indeed, mPTP opening can occur even at resting matrix  $[\text{Ca}^{2+}]$  if one of these other factors is changed sufficiently (Halestrap, 2009a,b). Phosphate, in particular, has been

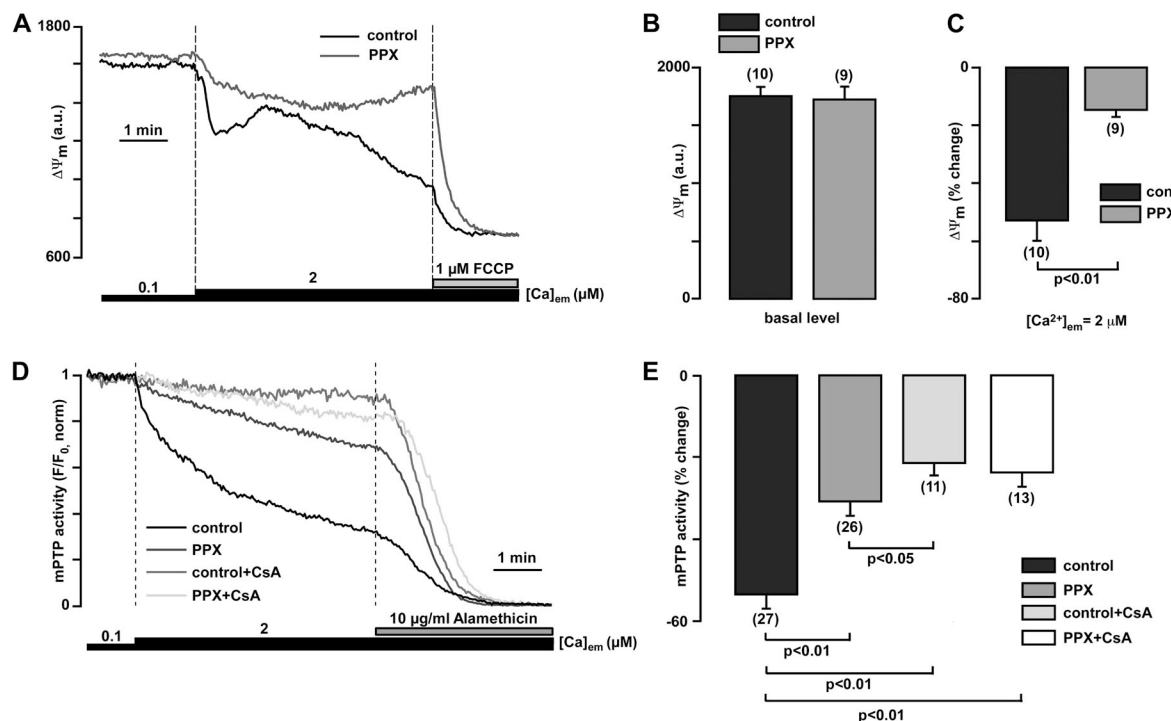


**Figure 5.** polyP depletion prevents opening of the permeability transition pore induced by mitochondrial  $\text{Ca}^{2+}$  overload. (A) Original recordings of TMRM fluorescence in permeabilized cells upon elevation of the  $[\text{Ca}^{2+}]_{\text{em}}$  from 0.1 to 2  $\mu\text{M}$ , and subsequent addition of 1  $\mu\text{M}$  FCCP in control (black) and polyP-depleted (PPX-expressing) myocytes (gray). (B) Average values reflecting the basal levels of TMRM fluorescence in control and PPX-expressing cells. (C) Average TMRM fluorescence decrease, measured at the end of exposure to 2  $\mu\text{M}$   $\text{Ca}^{2+}$  as percent decrease from initial levels in control and PPX-expressing cells. (D) Original recordings of calcein red fluorescence from permeabilized control (black), PPX-expressing (dark gray) and CsA-treated control (medium gray), and CsA-treated, PPX-expressing (light gray) cells. After permeabilization, cells were exposed to 2  $\mu\text{M}$   $\text{Ca}^{2+}$  in the presence or absence of CsA. To normalize calcein fluorescence, 10  $\mu\text{M}$  alamethicin was added at the end of the experiment to achieve the maximal calcein red release from mitochondria. (E) Summary of calcein red release (as percentage of total release obtained after alamethicin addition) from mitochondria measured at the end of 2- $\mu\text{M}$   $\text{Ca}^{2+}$  exposure in control, PPX-expressing, CsA-treated control cells, and CsA-treated, PPX-expressing cells.

referred to as an mPTP inducer since 1976 (Hunter et al., 1976); however, the mechanism of mPTP regulation by phosphate is not quite straightforward. First, by its ability to bind to protons, phosphate contributes to the maintenance of optimum pH levels for mPTP opening at  $\sim 7.3$  (Nicolli et al., 1993). Second, by decreasing matrix magnesium concentration, which competes with  $\text{Ca}^{2+}$  for a binding site on the mPTP and decreases its opening probability (Bernardi et al., 1992), phosphate would in fact facilitate mPTP opening (Di Lisa and Bernardi, 2009). A mitochondrial phosphate carrier was proposed as mPTP component recently (Leung et al., 2008), bringing more attention to the role of phosphates in mPTP activation. However, the ability of phosphate to buffer mitochondrial matrix  $\text{Ca}^{2+}$  will argue in the favor of phosphate as an mPTP inhibitor rather than mPTP inducer (Di Lisa and Bernardi, 2009). A recent study indicates that phosphate is actually required for inhibition of mPTP opening by CsA or genetic cyclophilin D ablation (Basso et al., 2008). The central aim of the present study was to investigate the contribution of inorganic polyP toward regulation of  $\text{Ca}^{2+}$ -induced mPTP activity in mitochondria of cardiac myocytes.

PolyP is a linear polymer of many tens to hundreds of  $\text{P}_i$  residues linked by high energy phosphoanhydride bonds similar to those found in ATP (Wood and Clark, 1988; Kornberg et al., 1999; Kulaev et al., 1999). PolyP is found in every cell in nature ranging from bacteria to mammals (Wood and Clark, 1988; Kornberg et al., 1999; Kulaev et al., 1999) and likely conserved from prebiotic times. Physiological roles of polyP are numerous and depend on size, concentration, and localization of the polymer. In mammalian cells, the concentration of polyP was found to be significantly lower compared with bacteria and yeast (Kumble and Kornberg, 1995; Kornberg et al., 1999). In bacteria, the majority of polyP is present in highly polymerized form of 800–1,000 residues and plays a role in energy (Wood and Clark, 1988; Kornberg et al., 1999; Kulaev et al., 1999) and phosphate (Kulaev et al., 1999) storage and as a chelator of heavy metals and  $\text{Ca}^{2+}$  (van Veen et al., 1993). Unlike bacteria, mammalian organisms contain mostly short-chain polyP, which is found in all tested organisms and tissues in various subcellular compartments (Kumble and Kornberg, 1995). Estimated levels of 25–120  $\mu\text{M}$  (in terms of phosphate residues) were detected in rodent tissues (brain, heart, kidney, liver, and lungs) (Kumble and Kornberg, 1995), in striking contrast to polyP levels of 50–120 mM detected in bacteria (*Escherichia coli*) and yeast (*Saccharomyces cerevisiae*) (Kornberg et al., 1999). In the present study (Fig. 1 A), we determined that polyP is present in mitochondria of rabbit hearts as a short-chain polymer with  $\sim 25$   $\text{P}_i$  groups. The amount of polyP in cardiac mitochondria was estimated to be  $280 \pm 60$  pmol/mg of protein. Taking into account that the total

matrix volume corresponding to 1 mg of mitochondrial protein is estimated to be  $1.6 \mu\text{l}$  (Schwerzmann et al., 1986), the upper limit of free polyP concentration is expected to be in the range of 200  $\mu\text{M}$ . This number is most likely an overestimate provided that most polyP is likely bound to other macromolecules. Because the amounts of polyP are relatively low, it is unlikely that polyP hydrolysis by PPX would result in significant changes in the total pool of mitochondrial  $\text{P}_i$ , the latter being a known modulator of mitochondrial function (Hunter et al., 1976; Di Lisa and Bernardi, 2009). This makes it rather unlikely that in cardiac myocytes polyP plays a significant role as  $\text{Ca}^{2+}$  and phosphate buffer. This notion is supported by our data presented in Figs. 2 and 3, where depletion of the mitochondrial polyP levels in rabbit cardiomyocytes affected neither the amplitude of electrically evoked cytosolic  $[\text{Ca}^{2+}]_i$  transients nor the magnitude of the mitochondrial  $\text{Ca}^{2+}$  uptake during moderate elevations of  $[\text{Ca}^{2+}]_{\text{em}}$ . However, the observed protective effect against  $\text{Ca}^{2+}$ -induced mPTP opening in polyP-depleted cells (Figs. 3–5) suggest a possible direct structural or regulatory role of polyP in mPTP induction rather than a  $\text{Ca}^{2+}$ /phosphate buffering function. This is consistent with previous reports where, with the exception of acidocalcisomes (Docampo et al., 2005), in mammalian organisms a primary role of polyP was linked to regulation of multiple processes through its interaction with organic polymers including proteins, DNA, RNA, and poly- $\beta$ -hydroxybutyrate (PHB) (Kornberg et al., 1999; Kulaev et al., 1999).

One of the most intriguing and yet to be answered questions regarding mPTP relates to the mechanism of mPTP activation by  $\text{Ca}^{2+}$ . The main conclusion that can be drawn from the experiments presented in Figs. 4 and 5 is that depletion of polyP leads to significant inhibition of  $\text{Ca}^{2+}$ -induced mPTP. The fact that polyP is a  $\text{Ca}^{2+}$ -binding polymer, and its depletion leads to inhibition of mPTP, allows us to propose that in fact, polyP might be the long-sought  $\text{Ca}^{2+}$  sensor of the mPTP.

The next important question is how polyP– $\text{Ca}^{2+}$  interaction would lead to the activation of mPTP. A possible explanation is that formation of polyP– $\text{Ca}^{2+}$  complexes in the presence of inorganic  $\text{P}_i$  would lead to the formation of aggregates that can be incorporated into the membrane and thus would induce an overall nonspecific increase in membrane permeability. This is somewhat similar to what occurs during  $\text{Ca}^{2+}$ – $\text{P}_i$ –DNA transfection in tissue culture cells (Castuma et al., 1995; Huang and Reusch, 1995). Although this model could explain an increase in membrane permeability, it cannot explain the fact that according to electrophysiological studies, mPTP is formed by a stable pore rather than a nonspecific increase in membrane permeability. Based on previous experimental data (Pavlov et al., 2005b), it is possible that formation of polyP– $\text{Ca}^{2+}$  can be directly related to the assembly and opening of the mPTP pore through the

formation of a polyP–Ca<sup>2+</sup>–PHB channel. This channel was first described in membranes of *E. coli* (Reusch and Sadoff, 1988), where the complex of polyP–PHB with the participation of Ca<sup>2+</sup> was proven to be responsible for the formation of channels required for exogenous DNA entry into *E. coli* cells competent for genetic transformation (Reusch and Sadoff, 1988; Castuma et al., 1995). In experiments with polyP–PHB–Ca<sup>2+</sup> complexes derived from *E. coli* (Reusch and Sadoff, 1988; Pavlov et al., 2005a) and with synthetic polymers (Das et al., 1997), the complex can form channels when reconstituted into lipid bilayers. Channels formed by polyP and PHB were found to be cationic selective with a preference for Ca<sup>2+</sup> and with ~100-pS conductance (Reusch and Sadoff, 1988; Castuma et al., 1995; Reusch et al., 1995; Das et al., 1997; Pavlov et al., 2005a). Most importantly, a similar polyP–PHB complex isolated from rat liver mitochondria (Pavlov et al., 2005b) can form large (mean maximal conductance of 500 pS in 150 KCl) voltage-dependent, weakly selective pores with multiple subconductances, including values of 100 pS. The behavior of this channel in the high conductance range, in many respects, mimicked the behavior of the mPTP seen in patch-clamp experiments of native mitochondria, suggesting an important physiological role (Pavlov et al., 2005b). We propose the possibility that the contribution of polyP to induction of mPTP opening might be explained by its Ca<sup>2+</sup>-mediated interactions with PHB.

Considering the fact that mPTP is a supra-molecular multiprotein complex and taking into account that PHB is known to be able to strongly interact with membrane proteins (Zakharian and Reusch, 2007; Negoda et al., 2010), we hypothesize that PHB of the polyP–Ca<sup>2+</sup>–PHB complex can closely associate with protein compounds of the mPTP. This association might provide a regulatory link between pore component of mPTP and its other structural and receptor proteins, most notably cyclophilin D. Alternatively, the activation of mPTP by Ca<sup>2+</sup>–polyP might involve direct Ca<sup>2+</sup>-mediated interactions between polyP and proteinaceous mPTP components without PHB involvement. Indeed, a similar mechanism has been shown recently for synthetic and natural polyanions that can bind to cytochrome c in the respiratory chain, rendering it inactive because of exclusion from its natural binding sites (Krasnikov et al., 2011).

In conclusion, our study demonstrates that mitochondrial polyP contributes toward mPTP opening in cardiac cells. In particular, we found that: (a) polyP is present in mitochondria of cardiac cells; (b) depletion of mitochondrial polyP does not affect cytosolic and mitochondrial Ca<sup>2+</sup> cycling; and (c) depletion of polyP inhibits Ca<sup>2+</sup>-induced mPTP opening in cardiomyocytes. These data demonstrate that polyP is a previously unrecognized critical activator of mPTP in cardiac cells.

We thank Drs. Robert Winkfein (University of Calgary) and Allen Samarel (Loyola University Chicago) for the help with the viral construct preparation.

This work was supported by the National Institutes of Health (grants HL62231, HL80101 and HL101235); the Leducq Foundation (to L.A. Blatter); the American Heart Association (AHA) National Scientist Development Grant (AHA 0735071N to E.N. Dedkova); Rush University Medical Center New Investigator Grant-in-Aid (31196 to E.N. Dedkova); and Heart and Stroke Foundation of Nova Scotia and Canadian Institute of Health Research (to E. Pavlov).

Edward N. Pugh Jr. served as editor.

Submitted: 10 February 2012

Accepted: 13 April 2012

## REFERENCES

Abramov, A.Y., C. Fraley, C.T. Diao, R. Winkfein, M.A. Colicos, M.R. Duchen, R.J. French, and E. Pavlov. 2007. Targeted polyphosphatase expression alters mitochondrial metabolism and inhibits calcium-dependent cell death. *Proc. Natl. Acad. Sci. USA*. 104:18091–18096. <http://dx.doi.org/10.1073/pnas.0708959104>

Aon, M.A., S. Cortassa, A.C. Wei, M. Grunnet, and B. O'Rourke. 2010. Energetic performance is improved by specific activation of K<sup>+</sup> fluxes through K(Ca) channels in heart mitochondria. *Biochim. Biophys. Acta*. 1797:71–80.

Aschar-Sobbi, R., A.Y. Abramov, C. Diao, M.E. Kargacin, G.J. Kargacin, R.J. French, and E. Pavlov. 2008. High sensitivity, quantitative measurements of polyphosphate using a new DAPI-based approach. *J. Fluoresc.* 18:859–866. <http://dx.doi.org/10.1007/s10895-008-0315-4>

Basso, E., V. Petronilli, M.A. Forte, and P. Bernardi. 2008. Phosphate is essential for inhibition of the mitochondrial permeability transition pore by cyclosporin A and by cyclophilin D ablation. *J. Biol. Chem.* 283:26307–26311. <http://dx.doi.org/10.1074/jbc.C800132200>

Bernardi, P., S. Vassanelli, P. Veronese, R. Colonna, I. Szabó, and M. Zoratti. 1992. Modulation of the mitochondrial permeability transition pore. Effect of protons and divalent cations. *J. Biol. Chem.* 267:2934–2939.

Bernardi, P., A. Krauskopf, E. Basso, V. Petronilli, E. Blachly-Dyson, F. Di Lisa, and M.A. Forte. 2006. The mitochondrial permeability transition from in vitro artifact to disease target. *FEBS J.* 273:2077–2099. <http://dx.doi.org/10.1111/j.1742-4658.2006.05213.x>

Bradford, M.M. 1976. A rapid and sensitive method for the quantitation of microgram quantities of protein utilizing the principle of protein-dye binding. *Anal. Biochem.* 72:248–254. [http://dx.doi.org/10.1016/0003-2697\(76\)90527-3](http://dx.doi.org/10.1016/0003-2697(76)90527-3)

Camara, A.K., M. Bienengraeber, and D.F. Stowe. 2011. Mitochondrial approaches to protect against cardiac ischemia and reperfusion injury. *Front Physiol.* 2:13. <http://dx.doi.org/10.3389/fphys.2011.00013>

Castuma, C.E., R. Huang, A. Kornberg, and R.N. Reusch. 1995. Inorganic polyphosphates in the acquisition of competence in *Escherichia coli*. *J. Biol. Chem.* 270:12980–12983. <http://dx.doi.org/10.1074/jbc.270.22.12980>

Cowling, R.T., and H.C. Birnboim. 1994. Incorporation of [<sup>32</sup>P] orthophosphate into inorganic polyphosphates by human granulocytes and other human cell types. *J. Biol. Chem.* 269:9480–9485.

Das, S., U.D. Lengweiler, D. Seebach, and R.N. Reusch. 1997. Proof for a nonproteinaceous calcium-selective channel in *Escherichia coli* by total synthesis from (R)-3-hydroxybutanoic acid and inorganic polyphosphate. *Proc. Natl. Acad. Sci. USA*. 94:9075–9079. <http://dx.doi.org/10.1073/pnas.94.17.9075>

Dedkova, E.N., and L.A. Blatter. 2005. Modulation of mitochondrial  $\text{Ca}^{2+}$  by nitric oxide in cultured bovine vascular endothelial cells. *Am. J. Physiol. Cell Physiol.* 289:C836–C845. <http://dx.doi.org/10.1152/ajpcell.00011.2005>

Dedkova, E.N., and L.A. Blatter. 2009. Characteristics and function of cardiac mitochondrial nitric oxide synthase. *J. Physiol.* 587:851–872. <http://dx.doi.org/10.1113/jphysiol.2008.165423>

Dedkova, E.N., and L.A. Blatter. 2012. Measuring mitochondrial function in intact cardiac myocytes. *J. Mol. Cell. Cardiol.* 52:48–61. <http://dx.doi.org/10.1016/j.jmcc.2011.08.030>

Di Lisa, F., and P. Bernardi. 2009. A CaPful of mechanisms regulating the mitochondrial permeability transition. *J. Mol. Cell. Cardiol.* 46:775–780. <http://dx.doi.org/10.1016/j.jmcc.2009.03.006>

Docampo, R., W. de Souza, K. Miranda, P. Rohloff, and S.N. Moreno. 2005. Acidocalcisomes—conserved from bacteria to man. *Nat. Rev. Microbiol.* 3:251–261. <http://dx.doi.org/10.1038/nrmicro1097>

Ferreira, R. 2010a. The reduction of infarct size—forty years of research. *Rev. Port. Cardiol.* 29:1037–1053.

Ferreira, R. 2010b. The reduction of infarct size—forty years of research—second of two parts. *Rev. Port. Cardiol.* 29:1219–1244.

Fiske, C.H., and Y. Subbarow. 1925. The colorimetric determination of phosphorus. *J. Biol. Chem.* 66:375–400.

Gomez, L., B. Li, N. Mewton, I. Sanchez, C. Piot, M. Elbaz, and M. Ovize. 2009. Inhibition of mitochondrial permeability transition pore opening: translation to patients. *Cardiovasc. Res.* 83:226–233. <http://dx.doi.org/10.1093/cvr/cvp063>

Halestrap, A.P. 2009a. Mitochondria and reperfusion injury of the heart—a holey death but not beyond salvation. *J. Bioenerg. Biomembr.* 41:113–121. <http://dx.doi.org/10.1007/s10863-009-9206-x>

Halestrap, A.P. 2009b. What is the mitochondrial permeability transition pore? *J. Mol. Cell. Cardiol.* 46:821–831. <http://dx.doi.org/10.1016/j.jmcc.2009.02.021>

Huang, R., and R.N. Reusch. 1995. Genetic competence in *Escherichia coli* requires poly-beta-hydroxybutyrate/calcium polyphosphate membrane complexes and certain divalent cations. *J. Bacteriol.* 177:486–490.

Hunter, D.R., R.A. Haworth, and J.H. Southard. 1976. Relationship between configuration, function, and permeability in calcium-treated mitochondria. *J. Biol. Chem.* 251:5069–5077.

Kawazoe, Y., S. Katoh, Y. Onodera, T. Kohgo, M. Shindoh, and T. Shiba. 2008. Activation of the FGF signaling pathway and subsequent induction of mesenchymal stem cell differentiation by inorganic polyphosphate. *Int. J. Biol. Sci.* 4:37–47. <http://dx.doi.org/10.7150/ijbs.4.37>

Kornberg, A., N.N. Rao, and D. Ault-Riché. 1999. Inorganic polyphosphate: a molecule of many functions. *Annu. Rev. Biochem.* 68:89–125. <http://dx.doi.org/10.1146/annurev.biochem.68.1.89>

Krasnikov, B.F., N.S. Melik-Nubarov, L.D. Zorova, A.E. Kuzminova, N.K. Isaev, A.J. Cooper, and D.B. Zorov. 2011. Synthetic and natural polyanions induce cytochrome c release from mitochondria in vitro and in situ. *Am. J. Physiol. Cell Physiol.* 300:C1193–C1203. <http://dx.doi.org/10.1152/ajpcell.00519.2009>

Kulaev, I., V. Vagabov, and T. Kulakovskaya. 1999. New aspects of inorganic polyphosphate metabolism and function. *J. Biosci. Bioeng.* 88:111–129. [http://dx.doi.org/10.1016/S1389-1723\(99\)80189-3](http://dx.doi.org/10.1016/S1389-1723(99)80189-3)

Kumble, K.D., and A. Kornberg. 1995. Inorganic polyphosphate in mammalian cells and tissues. *J. Biol. Chem.* 270:5818–5822. <http://dx.doi.org/10.1074/jbc.270.11.5818>

Leung, A.W., P. Varanyuwatana, and A.P. Halestrap. 2008. The mitochondrial phosphate carrier interacts with cyclophilin D and may play a key role in the permeability transition. *J. Biol. Chem.* 283:26312–26323. <http://dx.doi.org/10.1074/jbc.M805235200>

Marsh, D. 1996. Peptide models for membrane channels. *Biochem. J.* 315:345–361.

Meta, L., and C. Seitz. 1979. Isolation of mitochondria with emphasis on heart mitochondria from small amounts of tissue. *Methods Enzymol.* 55:39–46.

Morimoto, D., T. Tomita, S. Kuroda, C. Higuchi, S. Kato, T. Shiba, H. Nakagami, R. Morishita, and H. Yoshikawa. 2010. Inorganic polyphosphate differentiates human mesenchymal stem cells into osteoblastic cells. *J. Bone Miner. Metab.* 28:418–423. <http://dx.doi.org/10.1007/s00774-010-0157-4>

Müller, F., N.J. Mutch, W.A. Schenk, S.A. Smith, L. Esterl, H.M. Spronk, S. Schmidbauer, W.A. Gahl, J.H. Morrissey, and T. Renné. 2009. Platelet polyphosphates are proinflammatory and procoagulant mediators in vivo. *Cell.* 139:1143–1156. <http://dx.doi.org/10.1016/j.cell.2009.11.001>

Müller, W.E., X. Wang, B. Diehl-Seifert, K. Kropf, U. Schlossmacher, I. Lieberwirth, G. Glasser, M. Wiens, and H.C. Schröder. 2011. Inorganic polymeric phosphate/polyphosphate as an inducer of alkaline phosphatase and a modulator of intracellular  $\text{Ca}^{2+}$  level in osteoblasts (SaOS-2 cells) in vitro. *Acta Biomater.* 7:2661–2671. <http://dx.doi.org/10.1016/j.actbio.2011.03.007>

Negoda, A., E. Negoda, and R.N. Reusch. 2010. Importance of oligo-R-3-hydroxybutyrates to *S. lividans* KcsA channel structure and function. *Mol. Biosyst.* 6:2249–2255. <http://dx.doi.org/10.1039/c0mb00092b>

Nicolli, A., V. Petronilli, and P. Bernardi. 1993. Modulation of the mitochondrial cyclosporin A-sensitive permeability transition pore by matrix pH. Evidence that the pore open-closed probability is regulated by reversible histidine protonation. *Biochemistry.* 32:4461–4465. <http://dx.doi.org/10.1021/bi00067a039>

Omelon, S.J., and M.D. Grynpas. 2008. Relationships between polyphosphate chemistry, biochemistry and apatite biominerization. *Chem. Rev.* 108:4694–4715. <http://dx.doi.org/10.1021/cr0782527>

Omelon, S., J. Georgiou, Z.J. Henneman, L.M. Wise, B. Sukhu, T. Hunt, C. Wynnyckyj, D. Holmyard, R. Bielecki, and M.D. Grynpas. 2009. Control of vertebrate skeletal mineralization by polyphosphates. *PLoS ONE.* 4:e5634. <http://dx.doi.org/10.1371/journal.pone.00005634>

Pavlov, E., C. Grimble, C.T. Diao, and R.J. French. 2005a. A high-conductance mode of a poly-3-hydroxybutyrate/calcium/polyphosphate channel isolated from competent *Escherichia coli* cells. *FEBS Lett.* 579:5187–5192. <http://dx.doi.org/10.1016/j.febslet.2005.08.032>

Pavlov, E., E. Zakharian, C. Bladen, C.T. Diao, C. Grimble, R.N. Reusch, and R.J. French. 2005b. A large, voltage-dependent channel, isolated from mitochondria by water-free chloroform extraction. *Biophys. J.* 88:2614–2625. <http://dx.doi.org/10.1529/biophysj.104.057281>

Pavlov, E., R. Aschar-Sobbi, M. Campanella, R.J. Turner, M.R. Gómez-García, and A.Y. Abramov. 2010. Inorganic polyphosphate and energy metabolism in mammalian cells. *J. Biol. Chem.* 285:9420–9428. <http://dx.doi.org/10.1074/jbc.M109.013011>

Petronilli, V., G. Miotto, M. Canton, M. Brini, R. Colonna, P. Bernardi, and F. Di Lisa. 1999. Transient and long-lasting openings of the mitochondrial permeability transition pore can be monitored directly in intact cells by changes in mitochondrial calcein fluorescence. *Biophys. J.* 76:725–734. [http://dx.doi.org/10.1016/S0006-3495\(99\)77239-5](http://dx.doi.org/10.1016/S0006-3495(99)77239-5)

Piot, C., P. Croisille, P. Staat, H. Thibault, G. Rioufol, N. Mewton, R. Elbelghiti, T.T. Cung, E. Bonnefoy, D. Angoulvant, et al. 2008. Effect of cyclosporine on reperfusion injury in acute myocardial infarction. *N. Engl. J. Med.* 359:473–481. <http://dx.doi.org/10.1056/NEJMoa071142>

Rasola, A., and P. Bernardi. 2011. Mitochondrial permeability transition in  $\text{Ca}^{2+}$ -dependent apoptosis and necrosis. *Cell Calcium.* 50:222–233. <http://dx.doi.org/10.1016/j.ceca.2011.04.007>

Reusch, R.N., and H.L. Sadoff. 1988. Putative structure and functions of a poly-beta-hydroxybutyrate/calcium polyphosphate channel in bacterial plasma membranes. *Proc. Natl. Acad. Sci. USA*. 85:4176–4180. <http://dx.doi.org/10.1073/pnas.85.12.4176>

Reusch, R.N., R. Huang, and L.L. Bramble. 1995. Poly-3-hydroxybutyrate/polyphosphate complexes form voltage-activated  $\text{Ca}^{2+}$  channels in the plasma membranes of *Escherichia coli*. *Biophys. J.* 69:754–766. [http://dx.doi.org/10.1016/S0006-3495\(95\)79958-1](http://dx.doi.org/10.1016/S0006-3495(95)79958-1)

Ricchelli, F., J. Sileikytė, and P. Bernardi. 2011. Shedding light on the mitochondrial permeability transition. *Biochim. Biophys. Acta*. 1807:482–490. <http://dx.doi.org/10.1016/j.bbabi.2011.02.012>

Schwerzmann, K., L.M. Cruz-Orive, R. Eggman, A. Sänger, and E.R. Weibel. 1986. Molecular architecture of the inner membrane of mitochondria from rat liver: a combined biochemical and stereological study. *J. Cell Biol.* 102:97–103. <http://dx.doi.org/10.1083/jcb.102.1.97>

Sedova, M., E.N. Dedkova, and L.A. Blatter. 2006. Integration of rapid cytosolic  $\text{Ca}^{2+}$  signals by mitochondria in cat ventricular myocytes. *Am. J. Physiol. Cell Physiol.* 291:C840–C850. <http://dx.doi.org/10.1152/ajpcell.00619.2005>

Smith, S.A., and J.H. Morrissey. 2007. Sensitive fluorescence detection of polyphosphate in polyacrylamide gels using 4',6-diamidino-2-phenylindol. *Electrophoresis*. 28:3461–3465. <http://dx.doi.org/10.1002/elps.200700041>

van Veen, H.W., T. Abe, G.J. Kortstee, W.N. Konings, and A.J. Zehnder. 1993. Mechanism and energetics of the secondary phosphate transport system of *Acinetobacter johnsonii* 210A. *J. Biol. Chem.* 268:19377–19383.

Werkheiser, W.C., and W. Bartley. 1957. The study of steady-state concentrations of internal solutes of mitochondria by rapid centrifugal transfer to a fixation medium. *Biochem. J.* 66:79–91.

Wood, H.G., and J.E. Clark. 1988. Biological aspects of inorganic polyphosphates. *Annu. Rev. Biochem.* 57:235–260. <http://dx.doi.org/10.1146/annurev.bi.57.070188.001315>

Zakharian, E., and R.N. Reusch. 2007. *Haemophilus influenzae* outer membrane protein P5 is associated with inorganic polyphosphate and polyhydroxybutyrate. *Biophys. J.* 92:588–593. <http://dx.doi.org/10.1529/biophysj.106.095273>

Zakharian, E., B. Thyagarajan, R.J. French, E. Pavlov, and T. Rohacs. 2009. Inorganic polyphosphate modulates TRPM8 channels. *PLoS ONE*. 4:e5404. <http://dx.doi.org/10.1371/journal.pone.0005404>